The r-process nucleosynthesis during the decompression of neutron star crust material

S Goriely[1], A Bauswein[2], H-T Janka[2], S Panebianco[3], J-L Sida[3], J-F Lemaître[3], S Hilaire[4], N Dubray[4]

[1] Institut d'Astronomie et d'Astrophysique, ULB, CP226, 1050 Bruxelles, Belgium
[2] Max-Planck-Institut für Astrophysik, Postfach 1317, 85741 Garching, Germany
[3] CEA Saclay, Irfu/Service de Physique Nuclaire, 91191 Gif-sur-Yvette, France
[4] CEA, DAM, DIF, F-91297 Arpajon, France

E-mail: sgoriely@astro.ulb.ac.be

Abstract. About half of the nuclei heavier than iron observed in nature are produced by the so-called rapid neutron capture process, or r-process, of nucleosynthesis. The identification of the astrophysics site and the specific conditions in which the r-process takes place remains, however, one of the still-unsolved mysteries of modern astrophysics. Another underlying difficulty associated with our understanding of the r-process concerns the uncertainties in the predictions of nuclear properties for the few thousands exotic neutron-rich nuclei involved, for which essentially no experimental data exist.

The present paper emphasizes some important future challenges faced by nuclear physics in this problem, particularly in the determination of the nuclear structure properties of exotic neutron-rich nuclei as well as their radiative neutron capture rates and their fission probabilities. These quantities are particularly relevant to determine the composition of the matter resulting from the r-process. Both the astrophysics and the nuclear physics difficulties are critically reviewed with special attention paid to the r-process taking place during the decompression of neutron star matter following the merging of two neutron stars.

1. Introduction

The r-process of stellar nucleosynthesis is invoked to explain the production of the stable (and some long-lived radioactive) neutron-rich nuclides that are heavier than iron and observed in stars of various metallicities, as well as in the solar system (for a review, see [1]). In recent years nuclear astrophysicists have developed more and more sophisticated r-process models, trying to explain the solar system composition in a satisfactory way by adding new astrophysical or nuclear physics ingredients. However, the site(s) of the r-process has (have) not been identified yet and for this reason, the r-process nucleosynthesis remains one of the main puzzles of modern astrophysics.

Progress in the modelling of type-II supernovae and γ-ray bursts has raised a lot of excitement about the so-called neutrino-driven wind environment [1, 2, 3]. However, until now a successful r-process has not been obtained *ab initio* without tuning the relevant parameters (neutron excess, entropy, expansion timescale) in a way that is not supported by the most sophisticated existing models. Early in the development of the theory of nucleosynthesis, an alternative to the r-process in high-temperature supernova environments was proposed. It concerns the decompression

of cold neutronized matter. While such a connection was suggested decades ago [4, 5] and decompressed neutron star (NS) matter was found to be favorable for strong r-processing [6], only more recent and increasingly sophisticated hydrodynamic simulations could determine the ejecta mass to be about 10^{-3} to $10^{-2} M_\odot$ [7, 8, 9, 10, 11]. This mass, combined with the predicted astrophysical event rate (around $10^{-5}\,\mathrm{yr}^{-1}$ in the Milky Way [12]) can account for the majority of r-material in our Galaxy [10]. Nearly all of the ejecta are converted to r-process nuclei, whose radioactive decay heating leads to potentially observable electromagnetic radiation in the optical and infrared bands [13, 14] with 100–1000 times fainter peak brightnesses than those of typical supernovae and durations of only days [9, 10, 11, 15]. These "macronovae" or "kilonovae" are intensely searched for (with a recent, possible first success [16, 17]) and their unambiguous discovery would constitute the first detection of r-material in situ.

In the present contribution, we describe the r-process nucleosynthesis resulting from the decompression of NS crust material following the merging of two NSs and show that the predicted abundances can be in remarkable agreement with the solar r-abundance distribution for nuclei with $A > 140$ (Sect. 2). Sect 3 is devoted to the study of the sensitivity of the r-abundance prediction to some nuclear models, in particular nuclear masses and fission properties.

2. The r-process from NS mergers

Our NS–NS merger simulations were performed with a general relativistic Smoothed Particle Hydrodynamics scheme [11, 18, 19] representing the fluid by a set of particles with constant rest mass, whose hydrodynamical properties were evolved according to Lagrangian hydrodynamics, keeping the electron fraction of fluid elements fixed. The Einstein field equations were solved assuming a conformally flat spatial metric. It was shown in [11] that the r-abundance distributions resulting from binaries simulations with different mass ratios or different equation of state (EOS) were virtually identical. For this reason, in the present analysis, only the symmetric $1.35 M_\odot$–$1.35 M_\odot$ system with the DD2 EOS [20], including thermal effects, and a resolution of about 550,000 particles is considered. The mass ejected from the system is about $3\ 10^{-3} M_\odot$(see Ref. [19, 11] for more details on the gross properties of the ejecta, the influence of the EOS and the post-processing nucleosynthesis calculation). Note that the $1.35 M_\odot$–$1.35 M_\odot$ case is of particular interest since, according to population synthesis studies and pulsar observations, it represents the most abundant systems [21].

The r-process nucleosynthesis is calculated by post-processing the ejected mass elements taking into account their dynamics determined by the hydrodynamics simulation. The nucleosynthesis is followed with a reaction network including all 5000 species from protons up to Z=110 lying between the valley of β-stability and the neutron-drip line. All charged-particle fusion reactions on light and medium-mass elements that play a role when the nuclear statistical equilibrium freezes out are included in addition to radiative neutron captures and photodisintegrations. The reaction rates on light species are taken from the NETGEN library, which includes all the latest compilations of experimentally determined reaction rates [22]. Experimentally unknown reactions are estimated with the TALYS code [23, 24] on the basis of the Skyrme Hartree-Fock-Bogolyubov (HFB) nuclear mass model, HFB-21 [25]. On top of these reactions, β-decays as well as β-delayed neutron emission probabilities are also included, the corresponding rates being taken from the updated version of the Gross Theory [26] based on the same HFB-21 Q-values. Fission processes as well as α-decays are also included for all heavy species, as described in Sect. 3.2. In the present paper, we will restrict ourselves to study the sensitivity of the r-abundance calculation with respect to nuclear masses and fission properties.

In this specific r-process scenario, the number of free neutrons per seed nucleus is so high that the nuclear flow dominated by radiative neutron captures and β-decays follows the neutron-drip line. In tens of ms, the heaviest drip-line nuclei can be synthesized. However, according to microscopic predictions, neutron-induced, β-delayed as well as spontaneous fission become

efficient for drip-line nuclei with $Z \gtrsim 103$, prohibiting the formation of super-heavy nuclei and recycling the heavy material into lighter fragments, which will restart capturing the free neutrons. Such fission recycling can take place up to three times before the neutrons are exhausted. When the neutron density drops to some $N_n = 10^{20}$ cm^{-3}, the timescale of neutron capture by the most abundant nuclei with closed-shell neutron number $N = 126$ and $N = 184$ becomes longer than a few seconds, and the nuclear flow is dominated by β-decays back to the stability line, as well as fission and α-decay for the heaviest species.

The final abundance distribution of the matter ejected from a 1.35–1.35 $M_\odot$ NS merger on grounds of such a relativistic hydrodynamical simulation is shown in Fig. 1 and seen to be in remarkable agreement with the solar r-abundance distribution for nuclei with $A > 140$. The final composition of the ejecta is rather insensitive to details of the initial abundances and the astrophysical conditions, in particular the mass ratio of the two NSs, the quantity of matter ejected, and the EOS [10, 11, 27]. It should however be stressed that the distribution shown in Fig. 1 corresponds to the final composition of the ejecta mass-integrated over all mass elements found to be gravitationally unbound (about 1180 particles in this $1.35M_\odot$–$1.35M_\odot$ system). In our simulation, not all the mass elements lead to the same composition after ejection. Indeed, for a given binary system, mass elements can be ejected with relatively different velocities, so that the density evolution may vary significantly from one trajectory to the next. An example is given in Fig. 2 where it can be seen that fast expanding mass elements might not have time to capture all available free neutrons leading to no (trajectory 3) or only one fission cycle (trajectory 2) while the slowly expanding mass element (trajectory 1) allows for all free neutrons to be captured and three fission cycles to take place. If we define an expansion timescale as the time required for the density to drop from the initial drip density below the arbitrary value of 10^8g/cm^3, we find that for timescales shorter than typically ~ 5 ms no fission recycling takes place. In our relativistic simulations [10, 11], the integrated mass associated with a fast expansion remains small relative to the slowly expanding ones (Fig. 2, right panel), but their contributions to the final abundance distribution are found to be non-negligible, in particular around $A \simeq 200$, where their high abundances tend to fill the trough found in slowly expanding trajectories. For this reason, the Newtonian description of the NS merger hydrodynamics which tends to predict rather slow expansions [27] may give rise to different and unsatisfactory nucleosynthesis predictions. Note that the Newtonian simulations also present the drawback of overestimating the ejecta masses in general [8, 11, 27, 28].

Except for the sensitivity to the density history of the various mass elements ejected, the final abundance distribution remains extremely robust with respect to astrophysical conditions [11]. This robustness, which is compatible with the unique, solar-like abundance pattern of the elements heavier than Ba observed in metal-poor stars [29], supports the possible creation of these elements by fission recycling in NS merger ejecta. However, the estimated abundance distribution remains rather sensitive to the adopted nuclear models. The ejected material is composed almost exclusively of $A > 140$ nuclei, and in particular the $A \simeq 195$ third r-process peak appears in proportions similar to those observed in the solar system (Fig. 1), deviations resulting essentially from the still difficult task to predict neutron capture and β-decay rates for exotic neutron-rich nuclei. The situation for the lightest $110 \lesssim A \lesssim 170$ species has been rather unclear up to now and extremely dependent on fission properties, such as fission probabilities and fission fragment distributions (FFD). Indeed, the $110 \lesssim A \lesssim 170$ nuclei originate essentially from the spontaneous and β-delayed fission recycling that takes place in the $A \simeq 278$ region at the time all neutrons have been captured and the β-decays dominate the nuclear flow. The $A \simeq 278$ isobars correspond to the predominant abundance peak in the actinide region resulting from the turn-off point at the $N = 184$ drip-line shell closure, a bottleneck being created by β-decays along the nuclear flow during the irradiation phase. This specific mass region and its fission properties therefore play a key role for the production of the light species, as further

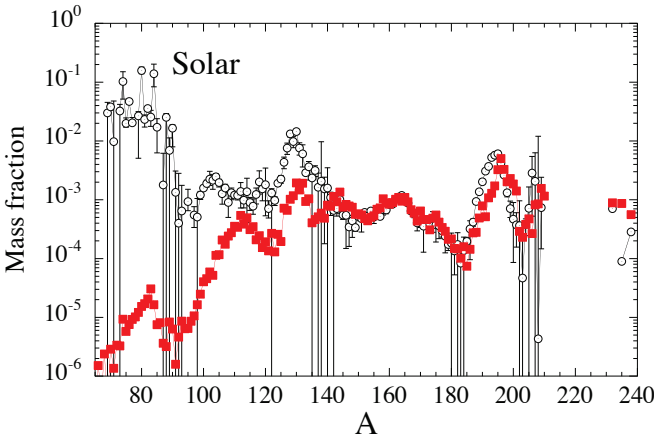

Figure 1. *Left*: Final abundance distribution of the matter ejected from the 1.35–1.35 $M_\odot$ NS merger as a function of the atomic mass. The distribution is normalized to the solar r-abundance distribution (dotted circles).

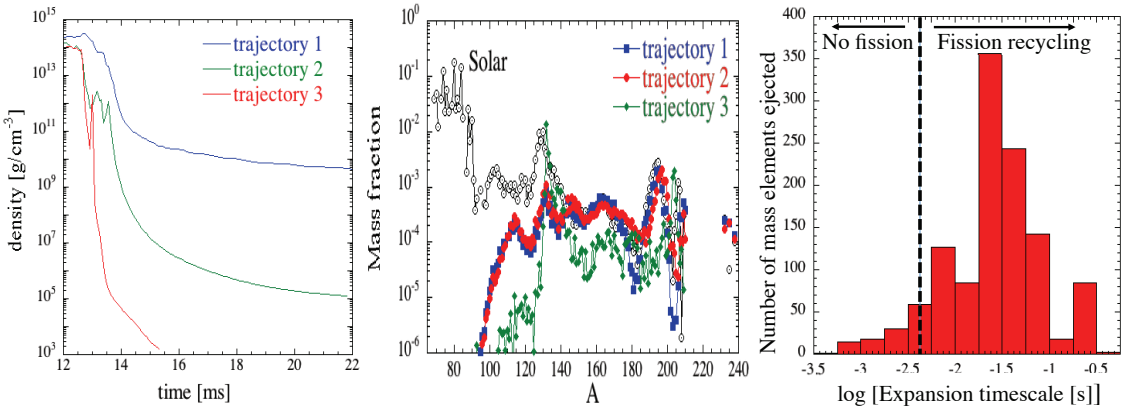

Figure 2. *Left*: Density evolution for three specific mass elements (trajectories) ejected from the 1.35–1.35 $M_\odot$ NS merger. *Middle*: Abundance distribution obtained for the same three trajectories, arbitrarily normalized to the solar system abundances (dotted circles).*Right*: Distribution of the expansion timescales for the 1180 mass elements ejected. The expansion timescale is defined here as the time required for the density to drop below the arbitrary value of 10^8g/cm^3.

discussed below.

3. Sensitivity to nuclear models

3.1. Nuclear mass models

Nuclear masses are known to be a fundamental ingredient for the r-process nucleosynthesis. They define the reaction and β-decay Q-values and consequently strongly affect the corresponding rates. During the decompression of the NS matter, the r-process dominantly takes place at low temperatures so that the radiative neutron capture is in competition with β-decays rather than with the photodisintegrations, as traditionally found in hot environments like in the ν-

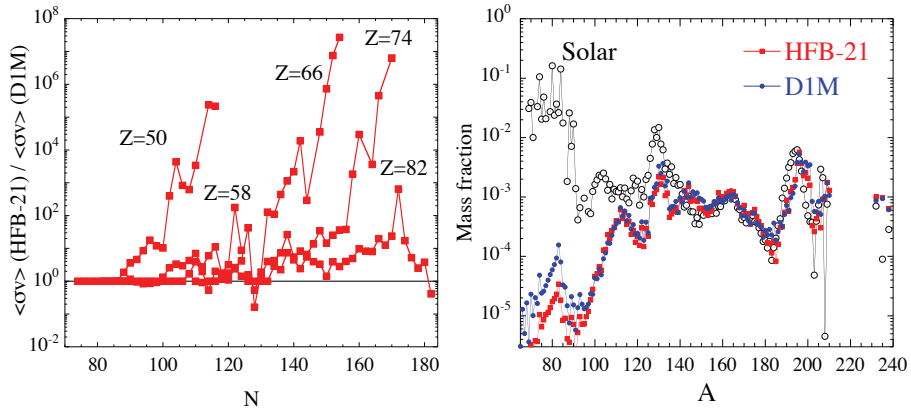

Figure 3. *Left*: Comparison between the neutron capture rates at a temperature $T = 10^9$ K for 5 isotopic chains obtained with the HFB-21 and D1M mass models. *Right*: Abundance distribution of the matter ejected from the 1.35–1.35 $M_\odot$ NS merger obtained with reaction rates calculated either with the HFB-21 or the D1M masses.

driven wind [1]. Reaction rates therefore fully enter the reaction network. We have studied the sensitivity of the nucleosynthesis calculation by considering the TALYS neutron capture rates estimated with two different sets of nuclear masses, namely HFB-21 masses based on the Skyrme Hartree-Fock-Bogolyubov (HFB) model [25] and D1M masses based on the Gogny HFB model [30]. The corresponding rates include a compound and a pre-equilibrium component but no direct capture contribution. Both sets of rates are compared in Fig. 3 (left panel) for five illustrative isotopic chains and seen to deviate up to a factor of 10^7 for drip line nuclei, the Skyrme HFB masses predicting essentially faster rates. However, such differences are seen in Fig. 3 (right panel) to have a rather small impact on the calculated r-abundances, deviations being restricted to the $A \simeq 180$ and $A \simeq 200$ regions. Note that the same β-decay rates [26] have been used in both nucleosynthesis calculations. Rather similar abundance distributions can be explained by the mass-averaging due to the large number of contributing trajectories, but also to the fact that the final distribution is shaped by the competition between neutron capture and β-decay for nuclei relatively close to the valley of β-stability at the time of the neutron freeze-out (see Ref. [1] for more details). Despite this similarity, more work on nuclear masses, but also on the determination of neutron capture (and also β-decay) rates is obviously needed, in particular to improve the prediction around the $A \simeq 195$ peak.

3.2. Fission

All fission rates, i.e the neutron-induced, photo-induced, β-delayed and spontaneous fission rates, have been estimated on the basis of the HFB-14 fission paths [31] and the nuclear level densities in the ground state as well as the saddle points within the combinatorial approach [32]. The neutron- and photo-induced fission rates have been estimated on the basis of the TALYS code for all nuclei with $90 \leq Z \leq 110$ [33]. Similarly, the β-delayed and spontaneous fission rates have been estimated with the same TALYS fission barrier penetration calculation. The β-delayed fission rate takes into account the full competition between the fission, neutron and photon channels, weighted by the population probability given by the β-decay strength function [34], i.e

$$\lambda_{\beta df} = \int_{B_f}^{Q_\beta} \frac{\Gamma_f}{\Gamma_f + \Gamma_n + \Gamma_\gamma} S_\beta(E) dE. \quad (1)$$

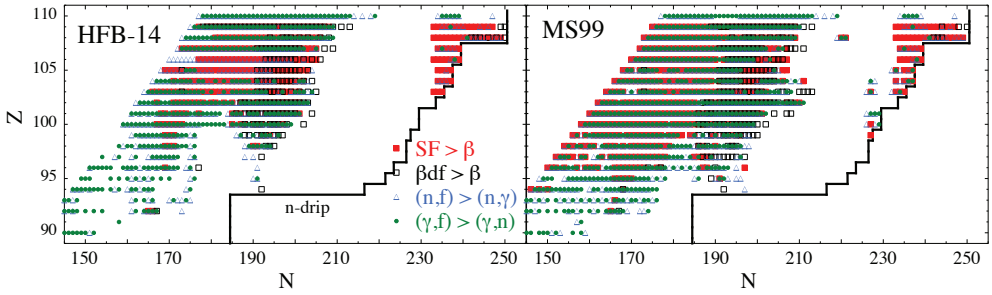

Figure 4. *Left*: Representation of dominant fission regions in the (N, Z) plane. Nuclei for which spontaneous fission (SF) is estimated to be faster than β-decays are shown by full squares, those for which β-delayed fission (βdf) is faster than β-decays by open squares, those for which neutron-induced fission (n,f) is faster than radiative neutron capture (n,γ) at $T = 10^9$ K by open triangles and those for which photofission (γ,f) at $T = 10^9$ K is faster than photoneutron emission (γ,n) by closed circles. For $Z = 110$, β-decay processes are not calculated. All fission probabilities are calculated with the HFB-14 fission paths [31]. *Right*: Same as the left panel when all fission probabilities are calculated with the MS99 fission barriers [35].

where B_f is the fission barrier, Q_β the β-decay Q-value and S_β the β-decay strength function estimated within the Gross Theory [34]. Γ_f, Γ_n, Γ_γ are the fission, neutron emission and electromagnetic de-excitation widths, respectively, at a given energy E which have been calculated consistently with the TALYS reaction code.

The spontaneous fission rate is deduced from the well-known formula $\lambda_{SF} = f_0 P$ where P is the barrier penetrability of the ground state calculated with the TALYS code and $f_0 = \omega_0/2\pi$ the frequency of oscillations in the fission mode for the ground state in the first well at the energy $\hbar\omega_0 \simeq 0.75$ MeV. The main fission regions by one of the four fission processes are illustrated in Fig. 4.

In order to perform sensitivity calculations, the fission probabilities have also been estimated on the basis of the Thomas-Fermi fission barriers compiled in Ref. [35] (hereafter MS99). To do so, the HFB-14 fission paths are renormalized so that the highest barrier corresponds now to the highest MS99 barrier. The latter usually predicts lower barriers than the mean-field approach so that many more nuclei are found to be affected by fission processes when use is made of the MS99 barriers, as shown in Fig. 4 (right panel). Note that MS99 barriers may not always be available for very exotic n-rich nuclei close to the neutron-drip line, especially for $Z \geq 106$. In this case, the HFB-14 barriers were adopted. This explains the relatively similar fissioning region for $Z \geq 103$ at the neutron drip line (Fig. 4). It is seen in Fig. 4 that if we adopt the HFB-14 fission barriers, during the freeze-out phase, fission takes place around $Z \simeq 101 - 102$ along the abundant $A = 278$ isobar, while the lower MS99 barriers [35] lead to fission already around the $Z \simeq 95 - 97$ isotopes.

Another ingredient of prime importance for the r-process nucleosynthesis is the fission FFD. The β-decay nuclei along the $A = 278$ isobar may fission either symmetrically or asymmetrically depending on the adopted model for the FFD. We consider here two models, namely the renewed statistical scission-point model based on microscopic ingredients called SPY [36] and the semi-empirical GEF model [37]. Both models differ not only in the prediction of the FFD for the exotic neutron-rich fissioning nuclei, but also in the estimate of the average number of emitted neutrons.

The final composition of the matter ejected from the 1.35–1.35 $M_\odot$ NS merger is shown

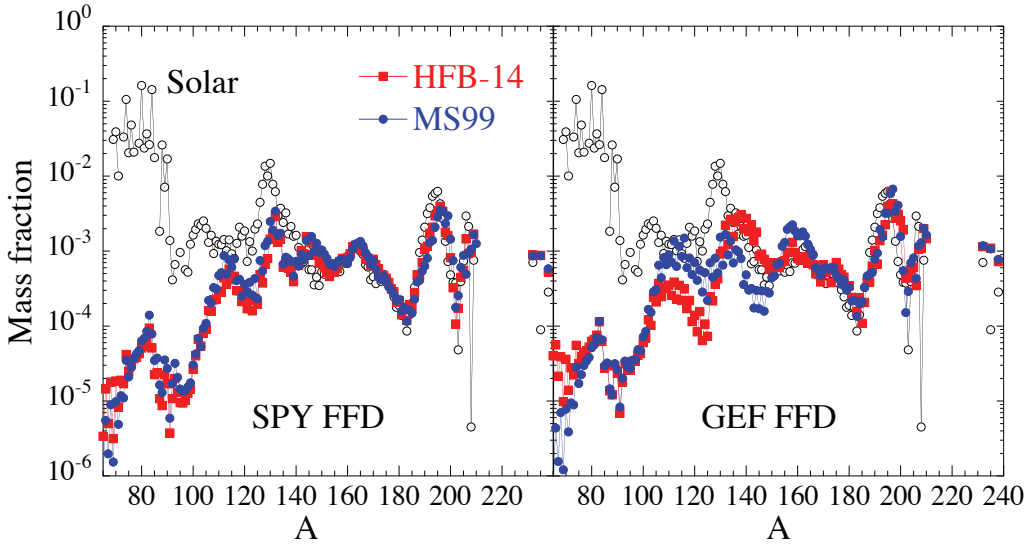

Figure 5. *Left*: Final abundance distribution of the matter ejected from the 1.35–1.35 $M_\odot$ NS merger as a function of the atomic mass. The distributions are normalized to the solar r-abundance distribution (dotted circles). The distributions are obtained with two sets of fission barriers, the HFB-14 [31] and MS99 barriers [35]. The adopted model for the FFD correspond to the SPY model [36]. *Right*: same as left panel when the FFD are estimated with the GEF model [37].

in Fig. 5 for fission rates obtained with both sets of fission barriers, namely the HFB-14 [31] and MS99 barriers [35] and two FFD models, namely the SPY [36] and GEF [37] models. As discussed above, the $A \simeq 278$ isobars that may fission during the freeze-out phase depend on the adopted fission model (see Fig. 4). Depending on the fissioning nuclei, they may fission either symmetrically or asymmetrically following the prediction of the FFD model. For example, considering the GEF FFD model, with the HFB-14 barriers, fission takes place symmetrically around $Z \simeq 101 - 102$ along the abundant $A = 278$ isobar, while the lower MS99 barriers [35] lead to fission already at the $Z \simeq 95 - 97$ isobar which are predicted to fission asymmetrically (see right panel of Fig. 5). In contrast, the SPY model predicts all $A = 278$ isobars to fission asymmetrically, leading to an abundance distribution rather insensitive to the adopted fission barriers (see left panel of Fig. 5). Interestingly, the SPY model can consistently explain the origin of the rare-earth peak by the r-process, in contrast to what is found with more phenomenological models predicting symmetrical mass yields for the $A \simeq 278$ fissioning nuclei.

4. Conclusions

Decompressed NS matter remains a viable site for the r-process, which is extremely robust with respect to many astrophysical uncertainties. This robustness, which is compatible with the unique, solar-like abundance pattern of the elements heavier than Ba observed in metal-poor stars, supports the possible creation of these elements by fission recycling in NS merger ejecta. However, the estimated abundance distribution remains rather sensitive to the adopted nuclear models. The ejected material is composed almost exclusively of $A > 140$ nuclei, and in particular the $A \simeq 195$ third r-process peak appears in proportions similar to those observed in the solar system, deviations resulting essentially from the still difficult task to predict neutron capture and β-decay rates for exotic neutron-rich nuclei. The situation for the lightest $110 \lesssim A \lesssim 170$ species has been rather unclear up to now and extremely dependent on fission properties, including in

particular the fission barriers and FFD. The newly derived FFD based on the SPY model can consistently explain the origin of the rare-earth peak by the r-process, in contrast to what is found with more phenomenological models predicting symmetrical mass yields for the $A \simeq 278$ fissioning nuclei. This new finding provides an even stronger hint that NS mergers could be a dominant process in the origin of the $A > 140$ r-nuclei in the Universe.

Acknowledgments

S.G. is F.R.S.-FNRS research associate and acknowledges the financial support of the "Actions de recherche concertées (ARC)" from the "Communauté française de Belgique". A.B. and H.-T.J. acknowledge support by DFG through grants SFB/TR7 and EXC 153.

References

[1] Arnould M, Goriely S and Takahashi K 2007 *Phys. Rep.* **450** 97
[2] Janka H-T 2012 *Ann. Rev. Nuc. Part. Science* **62** 407
[3] Wanajo S, Janka H-T and Müller B 2011 *Astrophys. J. Lett.* **726** L15
[4] Lattimer J M and Schramm D N 1974 *Astrophys. J.* **192** L145
[5] Eichler D, Livio M, Piran T and Schramm D N 1989 *Nature* **340** 126
[6] Meyer B S 1989 *Astrophys. J.* **343** 254
[7] Ruffert M, Janka H-T, Schäfer G 1996 *Astron. Astrophys.* **311** 532
[8] Rosswog S, Liebendörfer M, Thielemann F-K, Davies M B and Piran T 1999 *Astron. Astrophys.* **341** 499
[9] Roberts L F, Kasen D, Lee W H and Ramirez-Ruiz E 2011 *Astrophys. J. Lett.* **736** L2
[10] Goriely S, Bauswein A and Janka H-T 2011 *Astrophys. J. Lett.* **738** L32
[11] Bauswein A, Goriely S and Janka H-T 2013 *Astrophys. J.* **773** 78
[12] Dominik M, Belczynski K, Fryer C, Holz D E, Berti E, Bulik T, Mandel I and O'Shaughnessy R 2012 *Astrophys. J.* **759** 52
[13] Metzger B D, *et al.* 2010 *Month. Not. Roy. Astro. Soc.* **406** 2650
[14] Li L-X and Paczyński B 1998 *Astrophys. J.* **507** L59
[15] Barnes J and Kasen D 2013 *arXiv:1303.5787*
[16] Berger E, Fong W and Chornock R 2013 *arXiv:1306.3960*
[17] Tanvir N R, Levan A J, Fruchter A S, Hjorth J, Hounsell R A, Wiersema K, Tunnicliffe R L 2013 *Nature* 12505
[18] Oechslin R, Janka H-T and Marek A 2007 *Astron. Astrophys.* **467** 395
[19] Bauswein A, Janka H-T and Oechslin R 2010 *Phys. Rev. D* **82** 084043
[20] Typel S, Röpke G, Klähn T, Blaschke D and Wolter H. H. 2010 *Phys. Rev. C* **81** 015803
[21] Belczynski K, O'Shaughnessy R, Kalogera V, Rasio F, Taam R E and Bulik T 2008 *Astrophys. J. Lett.* **680** L129
[22] Xu Y, Goriely S, Jorissen A, Chen G L and Arnould M 2013 *Astron. Astrophys.* **549**, A10
[23] Koning A J, Hilaire S and Duijvestijn M C 2005 *Nuclear Data for Science and Technology* (eds. C. Haight et al.) AIP Conference **769** 1154
[24] Goriely S, Hilaire S and Koning A J 2008 *Astron. Astrophys.* **487** 76
[25] Goriely S, Chamel N and Pearson J M 2010 *Phys. Rev. C* **82** 035804
[26] Tachibana T, Yamada M and Yoshida Y 1990 *Prog. Theor. Phys.* **84** 64
[27] Korobkin O, Rosswog S, Arcones A and Winteler C 2012 *Month. Not. Roy. Astro. Soc.* **426** 1940
[28] Janka H-T, Eberl T, Ruffert M and Fryer C L 1999 *Astrophys. J. Lett.* **527** L39
[29] Sneden C, Cowan J J and Gallino R 2008 *Ann. Rev. Astron. & Astrophys.* **46** 241
[30] Goriely S, Hilaire S, Girod M and Péru S 2009 *Phys. Rev. Lett.* **102** 242501
[31] Goriely S, Samyn M and Pearson J M 2007 *Phys. Rev. C* **75** 064312
[32] Goriely S, Hilaire S and Koning A J 2008 *Phys. Rev. C 78* **064307**
[33] Goriely S, Hilaire S, Koning A J, Sin M and Capote R 2009 *Phys. Rev. C* **79** 024612
[34] Kodoma T and Takahashi K 1975 *Nucl. Phys. A.* **239** 48
[35] Myers W D and Swiatecki W J 1999 *Phys. Rev. C* **60** 014606
[36] Panebianco S, Sida J-L, Goutte H, Lemaître J-F, Dubray N and Hilaire S 2012 *Phys. Rev.* C **86** 064601
[37] Schmidt K-H and Jurado B 2010 *Phys. Rev. Lett.* **104** 212501